

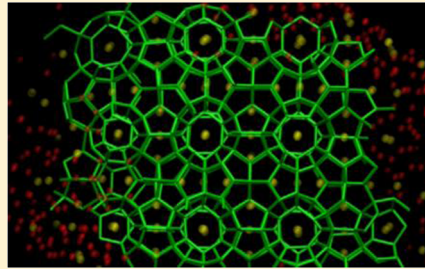
Nucleation of Gas Hydrates within Constant Energy Systems

Shuai Liang[†] and Peter G. Kusalik*

Department of Chemistry, University of Calgary, 2500 University Drive NW, Calgary, Alberta, Canada T2N 1N4

 Supporting Information

ABSTRACT: The early stage of formation of gas hydrates has recently attracted attention as amorphous intermediate gas hydrate structures have been observed, apparently contrary to a classical model of nucleation and some experimental observations. To date, essentially all reported molecular simulations of the nucleation of gas hydrates have been under constant temperature conditions, which does not consider the possible impacts of heat transfer on the nucleation processes. Here we show, using constant energy molecular simulations, that the nuclei at an early stage of the hydrate formation have relatively more crystalline order in comparison with those observed in previous isothermal (NPT or NVT) work. The current work suggests a more transient role for intermediate amorphous structures during hydrate nucleation, thereby providing a stronger link between molecular simulation and experimental observations. Our NVE results nevertheless support the two-step nucleation mechanism proposed in previous simulation studies under constant temperature conditions which features the initial formation of amorphous hydrate-like structures.



1. INTRODUCTION

Gas hydrates are ice-like crystalline compounds consisting of gas molecules each surrounded by a hydrogen-bonded cage formed by water molecules.^{1–3} These compounds are widely distributed in the world, store enormous amounts of methane, and have been recognized as a potential energy source for the future, although currently a number of technical challenges need to be overcome for economical extraction of natural gases.⁴ For the gas and oil industry, on the other hand, gas hydrates represent a major concern because they can form during gas and oil production in transport pipelines and can stop production and damage the pipelines and instruments, causing significant economic loss.⁵ The formation and dissociation of gas hydrates are also relevant to seafloor stability,⁶ global climate,^{7,8} and energy storage.^{9,10} Therefore, a thorough understanding of the mechanism of the hydrate nucleation and growth processes is of great interest both fundamentally and practically.

Different hypotheses have been proposed to describe the nucleation processes of gas hydrates. Christiansen and Sloan¹¹ have suggested a labile cluster mechanism, where the labile clusters are cage-like water clusters formed around individual gas molecules in solution. In this mechanism, crystalline gas hydrates form by agglomeration of these cage-like clusters. An alternative mechanism is the local structuring hypothesis proposed by Radhakrishnan and Trout,¹² which suggests that thermal fluctuations cause guest molecules to be arranged in configurations similar to that in gas hydrate phases that induce water molecules to adopt a hydrogen-bonded network close to that of gas hydrates. Recently, molecular dynamics (MD) simulation studies^{13–18} have suggested a two-step mechanism for the nucleation of gas hydrates, where the formation of crystalline gas hydrates from an aqueous gas solution exhibit an intermediate amorphous hydrate-like solid. Kusalik and co-

workers^{13,14} have shown that gas composition is a critical order parameter in determining the kinetics of the formation of the amorphous hydrate-like solids. They have demonstrated that the numbers of second neighbors of gas molecules (i.e., solvent separated gas molecules^{17–19}) in aqueous solution are an important factor in determining induction times for the nucleation of gas hydrates.¹⁴ More recently, Sarupria and Debenedetti¹⁶ have shown that under highly supersaturated conditions a uniform distribution of the gas molecules facilitates hydrate nucleation. Jacobson and Molinero¹⁵ have shown that crystalline hydrates can grow from an amorphous hydrate nucleus. Similar nucleation pathways have been observed with methane,^{13,20–24} hydrogen sulfide,¹⁴ and coarse-grained gas models^{15,17,18} in MD simulations. Liang and Kusalik²⁵ have observed that similar amorphous structures also appear near the solid/liquid interface during the crystal growth processes of gas hydrates. These MD studies strongly imply that the formation of crystalline gas hydrates involves amorphous structures as intermediates.

Experimentally, amorphous tetrahydrofuran (THF) hydrate solids have been prepared under a high pressure of ~1.3 GPa.²⁶ Bauer et al.²⁷ have developed an improved procedure to prepare purely amorphous THF hydrate. By removing any crystallinity detectable by powder X-ray diffraction, they show that the amorphous sample can sustain temperatures of at least 150 K without observing crystallization. On the other hand, by studying the water–CO₂ interface with X-ray reflectivity and diffraction²⁸ and liquid water/THF mixtures with X-ray Raman and Compton scattering,^{29,30} Lehmkühler and co-workers found no indication of the formation of amorphous gas hydrate

Received: August 23, 2012

Revised: January 16, 2013

Published: January 18, 2013

structures within the limits of their experimental resolutions. In contrast, the MD simulations with the coarse-grained model by Jacobson et al.¹⁵ suggest a rather high relative stability of the amorphous structures, with dissociation temperatures only about 10% lower than these of crystals.

To date, MD simulations of the nucleation of gas hydrate have been under constant temperature conditions (NPT^{13–18,20–22,24,31} or NVT^{21,24} ensembles), where the heat generated by hydrate formation is removed almost instantaneously by the operation of a thermostat coupled to the system. These studies have (implicitly) assumed that mass transfer plays a dominant role in determining the nucleation behavior of gas hydrates^{32–37} while heat transfer is less critical. Such an assumption is somewhat justified by the fact that nucleation is apparently a relatively slow process. Nevertheless, the heat released by gas hydrate formation may still increase the local temperature, and heat transfer away from the solid/liquid interface is required for further gas hydrate formation in real systems.

English and Phelan³⁸ have recognized the limitation of NPT simulations in realistically describing gas hydrate decomposition. Ripmeester, Alavi, and co-workers^{39–41} have performed MD simulations on methane hydrate dissociation under adiabatic, constant energy and volume (NVE), conditions. They have found that the heat consumed during hydrate dissociation and the heat transfer from the liquid to the hydrate phase play important roles in the molecular mechanism and rate of the decomposition.

Unlike the decomposition,^{16,39–42} the nucleation of gas hydrates are typically slow processes with long induction times. For example, the nucleation of CH₄ or CO₂ under relatively strong driving forces can take several microseconds.^{16,20,43–45} Long MD simulations however can generate cumulative errors in numerical integration that can cause a significant energy drift within NVE simulations. Therefore the direct simulation of CH₄ hydrates under constant energy conditions represents a current challenge. We have found that an aqueous H₂S solution can nucleate rather easily under relatively moderate driving forces.¹⁴ H₂S and CH₄ have similar molecular diameters (4.58 and 4.36 Å, respectively), and they typically form structure I (sI) hydrates,¹ where guest molecules occupy both the 5¹² and 5¹²6² cages of the sI hydrate crystals. As a result of these properties, H₂S hydrates can be expected to be a good model system to study the nucleation mechanism of (sI) hydrates.

In this paper, we report direct nucleation simulations of H₂S hydrates within constant energy systems. We observe temperature gradients between the nuclei formed and the solution phases as a result of the exothermic nucleation processes. These NVE simulations generate nuclei with more crystalline structures compared to those formed under constant temperature conditions. These results show that heat transfer can play an important role in the early stage of the nucleation of gas hydrates. The current NVE simulations do support the two-step nucleation mechanism^{13,14,17} which involves the formation of intermediate amorphous structures but suggest a more transient role for these amorphous structures.

2. METHODS

The simulation systems composed of 400 H₂S and 3312 H₂O molecules were prepared by melting a 3 × 4 × 6 H₂S hydrate crystal, where 400 randomly selected hydrate cages are filled with a H₂S molecule, at 350 K and 50 MPa for at least 20 ns. The production NVE runs were preceded by a short NPT

simulation of 100 ps to achieve the desired initial temperatures of 230 and 240 K. The pressure for the short NPT simulation was 50 MPa. Five independent NVE simulations were performed at each temperature. The sizes of the simulation box in the NVE runs can be found in the Supporting Information (SI). The gas/water ratio of the current systems is about 70% of that in a fully occupied sI H₂S hydrate crystal. Initially a small liquid H₂S bubble was found within the aqueous phase although it dissolved quickly into the solution as the nucleation progressed. Under the current conditions, the systems show almost instantaneous nucleation behavior¹⁴ and the conversion of the systems from liquid- to solid-like behavior is essentially completed within a time scale of a few tens of nanoseconds (as will be discussed later). To facilitate an analysis of the effect of the heat transfer on the nucleation behavior, five independent NPT simulations were also performed at each temperature and a pressure 50 MPa. To further confirm that volume fluctuations (or pressure changes during NVE simulations) play a minor role in determining nucleation behavior in the present systems, we performed 3 additional simulations under NVT conditions at 240 K (the sizes of the simulation box in the NVT runs can be found in the SI).

Throughout this work, water molecules are represented by the TIP4P/2005 potential model⁴⁶ and the H₂S molecules are represented by a four-site potential model.⁴⁷ The interactions between water and gas molecules were calculated as the usual sums of Coulomb and Lennard-Jones potentials. The cross terms for the Lennard-Jones parameters were determined using Lorentz–Berthelot mixing rules.⁴⁸ The equations of motion were integrated using velocity Verlet algorithms for translations and rotations.⁴⁹ A spherical cutoff of 11 Å was utilized for the short-ranged forces, while the electrostatic interactions were evaluated with the smooth particle mesh Ewald method.⁵⁰ A time step of 2 fs was used for the NPT and NVT simulations, whereas a smaller time step of 1 fs was used for the NVE simulations to increase the integration accuracies. Further details of the models and simulation methodologies can be found in the SI.

The molecular configurations presented in this work are averaged configurations with a sampling time of 100 ps.⁵¹ The water molecules are labeled as solid-like and liquid-like by their translational mean square displacements (MSD) with respect to the average molecular positions over the same time window (100 ps).^{25,52} The threshold value of MSD for molecular labeling is set as 0.24 Å², which has been determined by measuring the distribution function of MSD values of water molecules in a fully occupied sI hydrate crystal (see the SI). The F₄ structural order parameter⁵³ for each H₂O molecule was averaged over all neighboring H₂O molecules within 3.5 Å of the central molecule (see the SI for calculation details), where the molecular positions are the averaged positions over 100 ps time windows.^{25,52}

3. RESULTS AND DISCUSSION

Since the phase transition from liquid to solid is an exothermic process, a system will be heated during the nucleation and crystal growth processes. Figure 1 shows the overall temperatures of the systems during the NVE simulations, which are preceded by short NPT simulations at the desired temperatures of 230 (Figure 1a) and 240 K (Figure 1b). From Figure 1a, we can see that the temperatures increase from 230 to about 255–265 K as the simulations progress and reach apparent plateaus

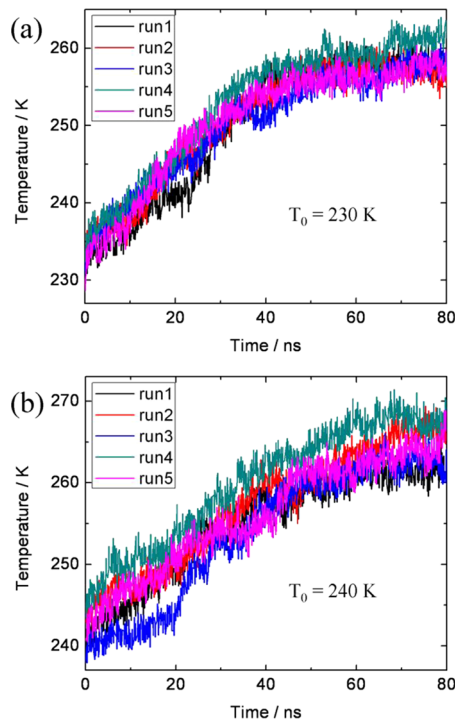


Figure 1. Evolution of temperatures of the system during NVE nucleation simulations starting at (a) 230 and (b) 240 K. Five independent trajectories are performed for each starting temperature (see legend).

within about 50 ns. The simulation trajectories starting at 240 K (Figure 1b) show similar behavior, and these systems reach temperature plateaus of about 260–270 K within about 60 ns. We note a smaller portion of the molecules form gas hydrate for the simulation trajectories starting at 240 K, emphasizing the influence of the temperature on the phase equilibrium between gas hydrate phases and the aqueous solutions. We again point out that at the starting temperature chosen for this work nucleation is essentially immediate.¹⁴

Figure 2 shows two examples of the time evolution of the potential, kinetic, and total system energies of NVE nucleation trajectories starting at 230 (Figure 2a) and 240 K (Figure 2b). The potential and kinetic energies show behavior consistent with that of the temperature shown in Figure 1. It is clearly evident that potential energy decreases and kinetic energy increases accompany the increase in the temperature of the system. The changes of the potential and kinetic energies are essentially canceled out during the whole trajectories, i.e., the total energy of the system remained virtually constant over the 80 ns simulations. For all of the NVE simulations performed in this work, the average drift in the total system energy is about 0.015 kJ/mol. Such an energy drift would correspond to only a 0.6 K temperature increase of the system if attributed entirely to the kinetic energy of the system. Therefore, the total system energies are reasonably conserved in the current NVE simulations. We note that the estimated energy drift (and hence temperature increase) would be more than 1 order of magnitude larger for a 1 μ s long simulation as in the case of the nucleation simulations of a CH₄ hydrate.^{16,20} Consequently, NVE simulations over microsecond time scales utilizing the present methodology would become potentially problematic considering that the nucleation rate of gas hydrates can vary significantly with a 5 K temperature difference.¹⁴

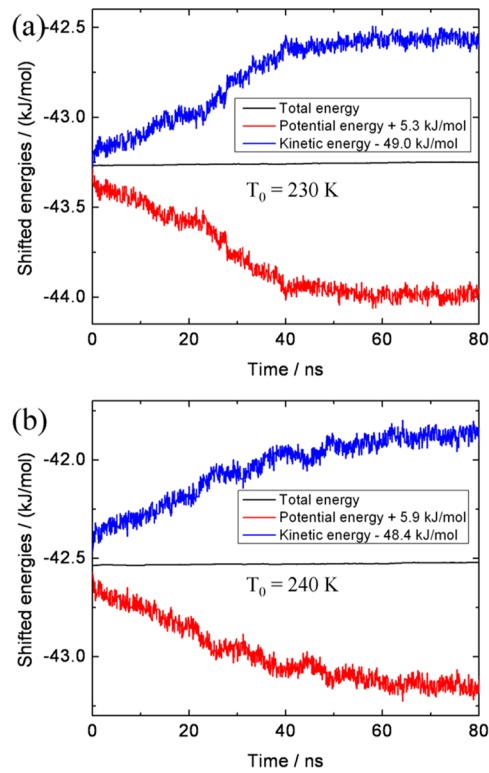


Figure 2. Evolution of the total energy, potential energy, and kinetic energy of the system during nucleation simulations starting at (a) 230 and (b) 240 K. The potential energy and kinetic energy are shifted to afford comparison (see legend).

With the isoenergetic simulation conditions, we observe temperature gradients form between the nuclei and the surrounding aqueous solution during the nucleation processes. Figure 3 show the temperature profile along the z direction of the system at 10 ns of a representative trajectory. Although there are relatively large fluctuations in this temperature profile, a temperature gradient of about 2 K is apparent in Figure 3. More examples of gradients can be found in the SI. We remark that corresponding temperature profiles obtained from NPT simulations show no evidence of a temperature gradient (see the SI). These results show that, although the nucleation of gas hydrates is a relatively slow process (i.e., occurring in a nanosecond time scale), small temperature gradients can still arise and may play important roles in the nucleation processes through alteration of the local temperature conditions. We note that the temperature profiles presented here were averaged over time windows of 100 ps and accumulated over 50 bins (slabs) along the z direction of the system; more spatially local temperature gradients may not easily be captured in MD simulations because of large fluctuations, but larger temperature gradients might be expected. These observations are consistent with the experimental study of crystallization of methane hydrates by Hwang et al.,⁵⁴ where they found that the heat released by CH₄ hydrate formation increases the temperature at the interface.

In comparison with the nucleation behavior under NPT conditions, the overall nucleation/crystallization rate for the NVE simulations appears somewhat slower during its early stage. Figure 4 shows the time evolution of the system-averaged F₄ structural order parameter⁵³ of two NVE nucleation trajectories, and NPT simulation results starting from the

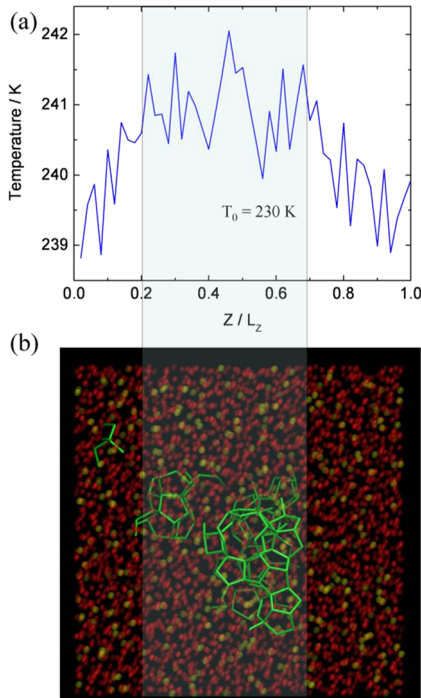


Figure 3. (a) Temperature profile along the z direction of the system at 10 ns for one NVE nucleation trajectory starting at 230 K. The temperatures are averaged over 100 ps and collected in 50 bins along the z direction. (b) The corresponding molecular configuration where the molecular positions are averaged over the same 100 ps time window. The H_2S molecules are represented by the yellow spheres. The water molecules are labeled as liquid-like and solid-like (see text), where liquid-like water molecules are represented by the red spheres and solid-like water molecules are connected by green lines. The H_2S and liquid-like water molecules are made transparent to emphasize the cage structures formed. The high temperature region is shaded in both the temperature profile and the corresponding molecular configuration to facilitate a direct comparison.

same configurations, where the relatively slower nucleation/crystallization rate of simulations under NVE conditions is apparent. Similar behavior has been observed in eight out of the total ten trajectories that were performed in this study (see the SI). We note that, if one compares results reported by Walsh et al.²⁴ for the induction times, nucleation rate, and the degree of solid-like clustering within aqueous methane solutions under NPT and NVT conditions, there are no significant differences. The results from our NVT simulations also appear very similar to the corresponding NPT simulations (see Figures S4–S6 in the SI). We believe that the relatively modest pressure changes observed during the NVE simulations (see the SI) have little influence on the nucleation behavior, as in a previous study¹⁴ we found no noticeable change in the nucleation behavior of H_2S hydrates within the pressure range of 0.5–50 MPa (at fixed system composition). The slight heating of the local region containing a nucleus will reduce the driving force for nucleation and hence is likely to be responsible for the slower nucleation/growth behavior.

The slight warming of the initial nuclei can be expected to enhance ordering/disordering fluctuations, and consequently structural reorganization within the nuclei appears easier, and more ordered crystalline structures are now possible within the NVE simulations. Figure 5 presents a couple of examples of nuclei exhibiting relatively more regular crystalline structures at

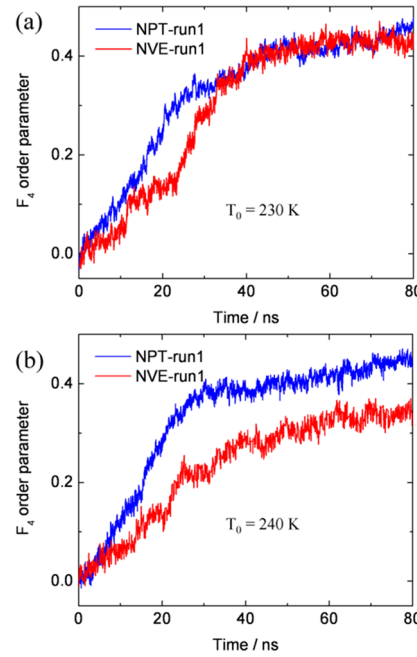


Figure 4. Evolution of the system-averaged F_4 order parameter (see text) of the water molecules during NVE nucleation simulations starting at (a) 230 and (b) 240 K. The evolution of the F_4 order parameters for corresponding NPT simulations starting from the same initial configuration are presented in each panel (see legend).

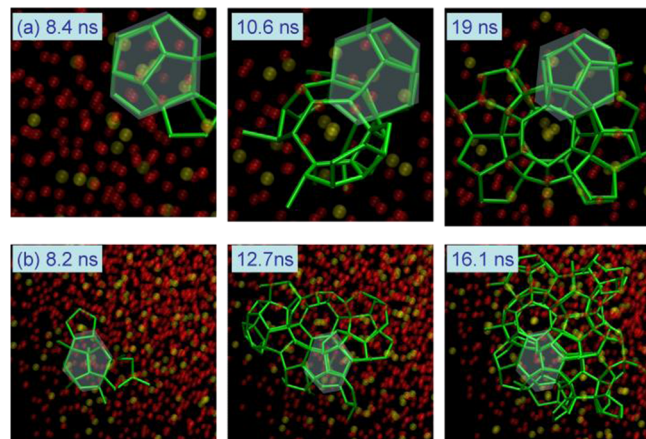


Figure 5. Molecular configurations showing the structural organization of the nuclei at specific stages of the NVE nucleation simulations. Images in a and b are from different trajectories, with the simulation time indicated in the legend. The molecules are represented and colored as in Figure 3. The shaded regions indicate the initial 5^{12} cage that formed during the nucleation.

early stages of the nucleation. Previous studies under NPT conditions^{14,18,22} have found that the initial cages that are formed are typically small 5^{12} cages and these cages tend to form around those gas molecules with a high degree of second-neighbor gas coordination. Hydrate nucleation then proceeds via the formation of face-sharing small 5^{12} cages.^{14,18,22} Here the initial cages that form in the NVE simulations are typically small 5^{12} cages as well, but the early stage structures appear to have more recognizable characteristics of regular crystalline structure. As shown in Figure 5, the structure of the nuclei can already be recognized as corresponding to a sl hydrate within 20 ns of the NVE simulations.

A few representative final molecular configurations from the constant energy trajectories are shown in Figure 6, where the

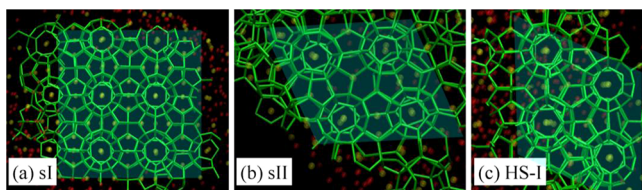


Figure 6. Molecular configurations showing the appearance of the regular (a) sI, (b) sII, and (c) HS-I gas hydrate structures within the solids formed during nucleation simulations under NVE conditions. The molecules are represented and colored as in Figure 3. The shaded regions indicate regular gas hydrate structures.

newly formed solids are in contact with the excess water within the system (see the Methods section). Although the detailed structures of the solids formed from different trajectories are different, they are typically hydrate-like, amorphous structures, where they feature reasonable short-ranged order. They include recognizable components of crystalline sI, sII, and HS-I^{20,55–57} hydrate structures (as shown in Figure 6a–c, respectively), as well as other irregular cage structures and unusual cage arrangements. These observations are similar to those reported in previous NPT simulations.^{13,14} In other words, the nucleation behavior observed here under NVE conditions also suggests that the nucleation of gas hydrates can be reasonably characterized by the two-step mechanism proposed previously,^{13,14,17} where the first step involves the relatively rapid formation of an amorphous hydrate-like solid and the second step involves the spontaneous evolution of the amorphous solid to a crystalline gas hydrate.

A notable observation from the current study is that, relative to previous nucleation simulations under constant temperature conditions,^{13–15,17,18,23,58,59} the solids that are formed here in NVE simulations tend to exhibit more crystalline order. To allow a more quantitative comparison of the crystalline order of these solids, we have measured the F_4 order parameters of only the solid-like molecules in the system. Figure 7 shows the F_4 order parameters of the final configurations of the 80 ns nucleation simulations under NVE and NPT conditions, where

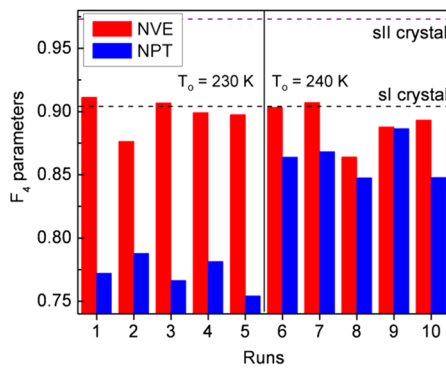


Figure 7. F_4 order parameters of the final configurations of 80 ns nucleation simulations under NVE and NPT conditions (see legend), where the parameters were averaged over the solid-like water molecules in the system. Runs 1–5 are started at 230 K, and runs 6–10 are started at 240 K. The F_4 parameters measured for fully occupied sI and sII crystals at 260 K are also shown in the figure (see legend).

the F_4 parameters have been averaged over the solid-like water molecules in the systems. We can see that, in general, the F_4 parameters of the configurations from NVE simulations have higher values than those from NPT simulations. Analysis of the structure within the early stage nuclei also consistently indicates that NVE simulations give rise to more ordered structures (see the SI). Additionally as already seen in Figure 6, relatively large domains of regular sI, sII, and HS-I crystalline structures form readily and with no additional annealing within NVE nucleation simulations. More final structures from the present simulations can be found in the SI. The higher degree of crystallinity within the solids formed within NVE trajectories suggests that the heat released during the formation of the gas hydrates can aid formation of more ordered structures within the initial nuclei. Since in isothermal (NPT or NVT) simulations^{13–15,17,18,23,58,59} the heat generated by hydrate formation is removed almost instantaneously by the operation of a thermostat, the structural evolution of a newly formed nucleus is apparently somewhat suppressed. Hence amorphous structures tend to be somewhat more prevalent in NPT simulations relative to those run under NVE conditions and started at the same temperature.

Finally, it is important to discuss the possible influences of the crystalline order within the early stage nuclei on the subsequent crystallization processes. The more ordered structures that tend to arise during nucleation in NVE simulations can subsequently be expected to anneal more rapidly. An example of cage annealing that is apparently enhanced by the presence of an ordered nucleus structure is shown in Figure 8. As can be seen in Figure 8a, a 5^{12} cage has

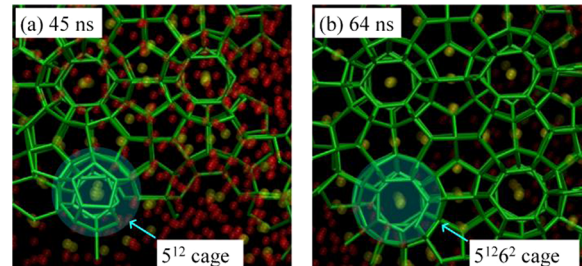


Figure 8. Molecular configurations showing cage reorganization during a nucleation simulation, where (a) a 5^{12} cage has formed at around 45 ns and (b) this cage has reorganized into a $5^{12}6^2$ cage within 20 ns (see legend). The molecules are represented and colored as in Figure 3.

been formed during this trajectory at about 45 ns. This 5^{12} cage is face-sharing with another 5^{12} cage, where such an arrangement does not conform to the local crystalline structure of sI gas hydrates. Within about 20 ns, this 5^{12} cage has converted to a $5^{12}6^2$ cage while several surrounding sI cage structures are also completed. It is clear that locally ordered structures are able to assist the annealing of other adjacent structures. Such observations are consistent with previous observations in hydrate crystal growth simulations.^{25,33,60–64} When provided a crystalline structural template, it is almost always crystalline gas hydrates growth that is observed on this template. Although disordered cage structures are occasionally seen behind the crystal growth front, such disordered cages are typically annealed to regular structures (which conform to the local crystalline structure) within 10 ns time frame.²⁵ We note that the mechanism whereby locally ordered structures facilitate

the annealing of adjacent structures holds generally for both constant temperature and constant energy ensembles. The more refined crystalline order observed for nuclei in the current NVE simulations apparently implies that amorphous solids will likely only form and exist in the very early stage of the nucleation and may help explain why these amorphous hydrate-like solids are not detectable by Compton scattering techniques.^{28–30}

4. CONCLUSIONS

In this work, we report molecular dynamics simulations of nucleation processes of gas hydrates under constant energy conditions. In comparison with simulation results under constant temperature conditions, we found that with the accumulation of the heat released during the nucleation process, which give rise to small local temperature gradients, the nucleation/crystallization rates within NVE simulations are generally slower during early stages of the nucleation. The initial nuclei observed in constant energy systems typically have a higher degree of crystalline order. Apparently the variation in temperature in both time and space, as can be observed in NVE simulations, can have important implication in the nucleation behavior observed for gas hydrates. The current NVE simulations do support the two-step nucleation mechanism proposed previously,^{13,14,17} featuring the rapid formation of amorphous hydrate-like structures that will subsequently anneal to crystalline solids. The more ordered nuclei that arise from the current simulations might be expected to anneal rather rapidly and hence could present a challenge for detection with current experimental techniques.

The setup of the current NVE simulations, which contain only a few thousand molecules and consequently do not allow heat exchange between a “system” and its “surroundings”, do not fully represent the conditions of most experimental studies. However, in comparison with simulations under constant temperature conditions (NPT or NVT) where the heat generated by gas hydrate formation is removed almost instantaneously by a thermostat coupled to the system, the current NVE simulations should more closely mimic experimental conditions in the early stages of the nucleation process. The temperature gradients observed in the current NVE simulations are qualitatively consistent with that observed in experimental studies. Additional more detailed and quantitative studies of the influences of the heat transfer on nucleation behavior are clearly warranted. It would be interesting, for example, to show in direct MD simulations further annealing of the solid structures formed under NVE conditions to regular hydrate crystals. Further studies aimed at tracking the evolution and quantifying the lifetime of the amorphous structures should consider relatively larger systems which represent a large thermal bath and where the crystalline phases should be able to form fully without the constraining influence of periodic boundaries. We note that Jacobson and Molinero¹⁵ have demonstrated that crystalline hydrates can grow out of an amorphous nuclei with a system of 54 000 coarse-grained particles. In future work a system of comparable or even larger size might be considered to explore more meaningfully the nucleation behavior of gas hydrates.

■ ASSOCIATED CONTENT

S Supporting Information

Details of the MD methodology, the evolution of pressures of the systems during NVE nucleation simulations, more examples

of the temperature profiles during the NVE nucleation processes, extensive comparisons of the nucleation behavior at early stages under the NPT and NVE conditions, and structures of the amorphous solids formed after 80 ns NVE simulations are available in supporting data. This material is available free of charge via the Internet at <http://pubs.acs.org>.

■ AUTHOR INFORMATION

Corresponding Author

*E-mail: peter.kusalik@ucalgary.ca.

Present Address

[†]Quantum Theory Project and Department of Chemistry, University of Florida, Gainesville, Florida, 32611 United States.

Notes

The authors declare no competing financial interest.

■ ACKNOWLEDGMENTS

We are grateful for the financial support of the Natural Sciences and Engineering Research Council of Canada. We also acknowledge computational resources made available via WestGrid (www.westgrid.ca) and the University of Calgary.

■ REFERENCES

- (1) Sloan, E. D.; Koh, C. A. *Clathrate Hydrates of Natural Gases*, 3rd ed.; CRC Press: Boca Raton, FL, 2008.
- (2) Sloan, E. D. Fundamental Principles and Applications of Natural Gas Hydrates. *Nature* **2003**, *426*, 353–359.
- (3) Buch, V.; Devlin, J. P.; Monreal, I. A.; Jagoda-Cwiklik, B.; Uras-Aytemiz, N.; Cwiklik, L. Clathrate Hydrates with Hydrogen-Bonding Guests. *Phys. Chem. Chem. Phys.* **2009**, *11*, 10245–10265.
- (4) Boswell, R. Is Gas Hydrate Energy within Reach? *Science* **2009**, *325*, 957–958.
- (5) Koh, C. A. Towards a Fundamental Understanding of Natural Gas Hydrates. *Chem. Soc. Rev.* **2002**, *31*, 157–167.
- (6) Kvenvolden, K. A. Potential Effects of Gas Hydrate on Human Welfare. *Proc. Natl. Acad. Sci. U.S.A.* **1999**, *96*, 3420–3426.
- (7) Bohannon, J. Energy—Weighing the Climate Risks of an Untapped Fossil Fuel. *Science* **2008**, *319*, 1753–1753.
- (8) McElwain, J. C.; Wade-Murphy, J.; Hesselbo, S. P. Changes in Carbon Dioxide During an Oceanic Anoxic Event Linked to Intrusion into Gondwana Coals. *Nature* **2005**, *435*, 479–482.
- (9) Lee, H.; Lee, J. W.; Kim, D. Y.; Park, J.; Seo, Y. T.; Zeng, H.; Moudrakovski, I. L.; Ratcliffe, C. I.; Ripmeester, J. A. Tuning Clathrate Hydrates for Hydrogen Storage. *Nature* **2005**, *434*, 743–746.
- (10) Florusse, L. J.; Peters, C. J.; Schoonman, J.; Hester, K. C.; Koh, C. A.; Dec, S. F.; Marsh, K. N.; Sloan, E. D. Stable Low-Pressure Hydrogen Clusters Stored in a Binary Clathrate Hydrate. *Science* **2004**, *306*, 469–471.
- (11) Christiansen, R. L.; Sloan, E. D. Mechanisms and Kinetics of Hydrate Formation. *Ann. N. Y. Acad. Sci.* **1994**, *715*, 283–305.
- (12) Radhakrishnan, R.; Trout, B. L. A New Approach for Studying Nucleation Phenomena Using Molecular Simulations: Application to CO₂ Hydrate Clathrates. *J. Chem. Phys.* **2002**, *117*, 1786–1796.
- (13) Vatamanu, J.; Kusalik, P. G. Observation of Two-Step Nucleation in Methane Hydrates. *Phys. Chem. Chem. Phys.* **2010**, *12*, 15065–15072.
- (14) Liang, S.; Kusalik, P. G. Exploring Nucleation of H₂S Hydrates. *Chem. Sci.* **2011**, *2*, 1286–1292.
- (15) Jacobson, L. C.; Molinero, V. Can Amorphous Nuclei Grow Crystalline Clathrates? Size and Crystallinity of Critical Clathrate Nuclei. *J. Am. Chem. Soc.* **2011**, *133*, 6458–6463.
- (16) Sarupria, S.; Debenedetti, P. G. Homogeneous Nucleation of Methane Hydrate in Microsecond Molecular Dynamics Simulations. *J. Phys. Chem. Lett.* **2012**, *3*, 2942–2947.

- (17) Jacobson, L. C.; Hujo, W.; Molinero, V. Amorphous Precursors in the Nucleation of Clathrate Hydrates. *J. Am. Chem. Soc.* **2010**, *132*, 11806–11811.
- (18) Jacobson, L. C.; Hujo, W.; Molinero, V. Nucleation Pathways of Clathrate Hydrates: Effect of Guest Size and Solubility. *J. Phys. Chem. B* **2010**, *114*, 13796–13807.
- (19) Matsumoto, M. Four-Body Cooperativity in Hydrophonic Association of Methane. *J. Phys. Chem. Lett.* **2010**, *1*, 1552–1556.
- (20) Walsh, M. R.; Koh, C. A.; Sloan, E. D.; Sum, A. K.; Wu, D. T. Microsecond Simulations of Spontaneous Methane Hydrate Nucleation and Growth. *Science* **2009**, *326*, 1095–1098.
- (21) Walsh, M. R.; Rainey, J. D.; Lafond, P. G.; Park, D.-H.; Beckham, G. T.; Jones, M. D.; Lee, K.-H.; Koh, C. A.; Sloan, E. D.; Wu, D. T.; Sum, A. K. The Cages, Dynamics, and Structuring of Incipient Methane Clathrate Hydrates. *Phys. Chem. Phys. Chem.* **2011**, *13*, 19951–19959.
- (22) Hawtin, R. W.; Quigley, D.; Rodger, P. M. Gas Hydrate Nucleation and Cage Formation at a Water/Methane Interface. *Phys. Chem. Chem. Phys.* **2008**, *10*, 4853–4864.
- (23) Guo, G. J.; Zhang, Y. G.; Liu, C. J.; Li, K. H. Using the Face-Saturated Incomplete Cage Analysis to Quantify the Cage Compositions and Cage Linking Structures of Amorphous Phase Hydrates. *Phys. Chem. Chem. Phys.* **2011**, *13*, 12048–12057.
- (24) Walsh, M. R.; Beckham, G. T.; Koh, C. A.; Sloan, E. D.; Wu, D. T.; Sum, A. K. Methane Hydrate Nucleation Rates from Molecular Dynamics Simulations: Effects of Aqueous Methane Concentration, Interfacial Curvature, and System Size. *J. Phys. Chem. C* **2011**, *115*, 21241–21248.
- (25) Liang, S.; Kusalik, P. G. Explorations of Gas Hydrate Crystal Growth by Molecular Simulations. *Chem. Phys. Lett.* **2010**, *494*, 123–133.
- (26) Suzuki, Y. Evidence of Pressure-Induced Amorphization of Tetrahydrofuran Clathrate Hydrate. *Phys. Rev. B* **2004**, *70*, 172108.
- (27) Bauer, M.; Tobbens, D. M.; Mayer, E.; Loerting, T. Pressure-Amorphized Cubic Structure II Clathrate Hydrate: Crystallization in Slow Motion. *Phys. Chem. Chem. Phys.* **2011**, *13*, 2167–2171.
- (28) Lehmkuhler, F.; Paulus, M.; Sternemann, C.; Lietz, D.; Venturini, F.; Gutt, C.; Tolan, M. The Carbon Dioxide-Water Interface at Conditions of Gas Hydrate Formation. *J. Am. Chem. Soc.* **2009**, *131*, 585–589.
- (29) Conrad, H.; Lehmkuhler, F.; Sternemann, C.; Sakko, A.; Paschek, D.; Simonelli, L.; Huotari, S.; Feroughi, O.; Tolan, M.; Hamalainen, K. Tetrahydrofuran Clathrate Hydrate Formation. *Phys. Rev. Lett.* **2009**, *103*, 218301.
- (30) Lehmkuhler, F.; Sakko, A.; Steinke, I.; Sternemann, C.; Hakala, M.; Sahle, C. J.; Buslaps, T.; Simonelli, L.; Galambosi, S.; Paulus, M.; Pylkkanen, T.; Tolan, M.; Hamalainen, K. Temperature-Induced Structural Changes of Tetrahydrofuran Clathrate and of the Liquid Water/Tetrahydrofuran Mixture. *J. Phys. Chem. C* **2011**, *115*, 21009–21015.
- (31) Nguyen, A. H.; Jacobson, L. C.; Molinero, V. Structure of the Clathrate/Solution Interface and Mechanism of Cross-Nucleation of Clathrate Hydrates. *J. Phys. Chem. C* **2012**, *116*, 19828–19838.
- (32) Rivera, J. J.; Janda, K. C. Ice Particle Size and Temperature Dependence of the Kinetics of Propane Clathrate Hydrate Formation. *J. Phys. Chem. C* **2012**, *116*, 19062–19072.
- (33) Liang, S.; Kusalik, P. G. The Mobility of Water Molecules through Gas Hydrates. *J. Am. Chem. Soc.* **2011**, *133*, 1870–1876.
- (34) Davies, S. R.; Lachance, J. W.; Sloan, E. D.; Koh, C. A. High-Pressure Differential Scanning Calorimetry Measurements of the Mass Transfer Resistance across a Methane Hydrate Film as a Function of Time and Subcooling. *Ind. Eng. Chem. Res.* **2010**, *49*, 12319–12326.
- (35) Davies, S. R.; Sloan, E. D.; Sum, A. K.; Koh, C. A. In situ Studies of the Mass Transfer Mechanism across a Methane Hydrate Film Using High-Resolution Confocal Raman Spectroscopy. *J. Phys. Chem. C* **2010**, *114*, 1173–1180.
- (36) Falenty, A.; Genov, G.; Hansen, T. C.; Kuhs, W. F.; Salamatian, A. N. Kinetics of CO₂ Hydrate Formation from Water Frost at Low Temperatures: Experimental Results and Theoretical Model. *J. Phys. Chem. C* **2011**, *115*, 4022–4032.
- (37) Jin, Y.; Konno, Y.; Nagao, J. Growth of Methane Clathrate Hydrates in Porous Media. *Energy Fuels* **2012**, *26*, 2242–2247.
- (38) English, N. J.; Phelan, G. M. Molecular Dynamics Study of Thermal-Driven Methane Hydrate Dissociation. *J. Chem. Phys.* **2009**, *131*, 074704.
- (39) Alavi, S.; Ripmeester, J. A. Nonequilibrium Adiabatic Molecular Dynamics Simulations of Methane Clathrate Hydrate Decomposition. *J. Chem. Phys.* **2010**, *132*, 144703.
- (40) Bagherzadeh, S. A.; Englezos, P.; Alavi, S.; Ripmeester, J. A. Molecular Simulation of Non-Equilibrium Methane Hydrate Decomposition Process. *J. Chem. Thermodyn.* **2012**, *44*, 13–19.
- (41) Bagherzadeh, S. A.; Englezos, P.; Alavi, S.; Ripmeester, J. A. Molecular Modeling of the Dissociation of Methane Hydrate in Contact with a Silica Surface. *J. Phys. Chem. B* **2012**, *116*, 3188–3197.
- (42) Liu, Y.; Zhao, J.; Xu, J. Dissociation Mechanism of Carbon Dioxide Hydrate by Molecular Dynamic Simulation and Ab Initio Calculation. *Comput. Theor. Chem.* **2012**, *991*, 165–173.
- (43) Bai, D.; Chen, G.; Zhang, X.; Wang, W. Nucleation of the CO₂ Hydrate from Three-Phase Contact Lines. *Langmuir* **2012**, *28*, 7730–7736.
- (44) Bai, D.; Chen, G.; Zhang, X.; Wang, W. Microsecond Molecular Dynamics Simulations of the Kinetic Pathways of Gas Hydrate Formation from Solid Surfaces. *Langmuir* **2011**, *27*, 5961–5967.
- (45) Knott, B. C.; Molinero, V.; Doherty, M. F.; Peters, B. Homogeneous Nucleation of Methane Hydrates: Unrealistic under Realistic Conditions. *J. Am. Chem. Soc.* **2012**, *134*, 19544–19547.
- (46) Abascal, J. L. F.; Vega, C. A General Purpose Model for the Condensed Phases of Water: Tip4p/2005. *J. Chem. Phys.* **2005**, *123*, 234505.
- (47) Forester, T. R.; McDonald, I. R.; Klein, M. L. Intermolecular Potentials and the Properties of Liquid and Solid Hydrogen-Sulfide. *Chem. Phys.* **1989**, *129*, 225–234.
- (48) Allen, M. P.; Tildesley, D. J. *Computer Simulation of Liquids*; Oxford University Press: Oxford, U.K., 1989.
- (49) Rozmanov, D.; Kusalik, P. G. Robust Rotational-Velocity-Verlet Integration Methods. *Phys. Rev. E* **2010**, *81*, 056706.
- (50) Essmann, U.; Perera, L.; Berkowitz, M. L.; Darden, T.; Lee, H.; Pedersen, L. G. A Smooth Particle Mesh Ewald Method. *J. Chem. Phys.* **1995**, *103*, 8577–8593.
- (51) Razul, M. S. G.; Hendry, J. G.; Kusalik, P. G. Mechanisms of Heterogeneous Crystal Growth in Atomic Systems: Insights from Computer Simulations. *J. Chem. Phys.* **2005**, *123*, 204722.
- (52) Vatamanu, J.; Kusalik, P. G. Molecular Dynamics Methodology to Investigate Steady-State Heterogeneous Crystal Growth. *J. Chem. Phys.* **2007**, *126*, 124703.
- (53) Rodger, P. M.; Forester, T. R.; Smith, W. Simulations of the Methane Hydrate Methane Gas Interface near Hydrate Forming Conditions. *Fluid Phase Equilib.* **1996**, *116*, 326–332.
- (54) Hwang, M. J.; Wright, D. A.; Kapur, A.; Holder, G. D. An Experimental-Study of Crystallization and Crystal-Growth of Methane Hydrates from Melting Ice. *J. Inclusion Phenom. Mol. Recognit. Chem.* **1990**, *8*, 103–116.
- (55) Vatamanu, J.; Kusalik, P. G. Unusual Crystalline and Polycrystalline Structures in Methane Hydrates. *J. Am. Chem. Soc.* **2006**, *128*, 15588–15589.
- (56) Yang, L.; Tulk, C. A.; Klug, D. D.; Moudrakovski, I. L.; Ratcliffe, C. I.; Ripmeester, J. A.; Chakoumakos, B. C.; Ehm, L.; Martin, C. D.; Parise, J. B. Synthesis and Characterization of a New Structure of Gas Hydrate. *Proc. Natl. Acad. Sci. U.S.A.* **2009**, *106*, 6060–6064.
- (57) Jeffrey, G. A. *Comprehensive Supramolecular Chemistry*; Atwood, J. L., Davies, J. E. D., MacNicol, D. D., Vogtle, F., Lehn, J. M., Eds.; Pergamon: Oxford, New York, 1996; Vol. 6.
- (58) Jacobson, L. C.; Matsumoto, M.; Molinero, V. Order Parameters for the Multistep Crystallization of Clathrate Hydrates. *J. Chem. Phys.* **2011**, *135*, 074501.

- (59) Liang, S.; Rozmanov, D.; Kusalik, P. G. Crystal Growth Simulations of Methane Hydrates in the Presence of Silica Surfaces. *Phys. Chem. Chem. Phys.* **2011**, *13*, 19856–19864.
- (60) Liang, S.; Kusalik, P. G. Crystal Growth Simulations of H₂S Hydrate. *J. Phys. Chem. B* **2010**, *114*, 9563–9571.
- (61) Vatamanu, J.; Kusalik, P. G. Molecular Insights into the Heterogeneous Crystal Growth of sI Methane Hydrate. *J. Phys. Chem. B* **2006**, *110*, 15896–15904.
- (62) Vatamanu, J.; Kusalik, P. G. Heterogeneous Crystal Growth of Methane Hydrate on Its sII [001] Crystallographic Face. *J. Phys. Chem. B* **2008**, *112*, 2399–2404.
- (63) Tung, Y. T.; Chen, L. J.; Chen, Y. P.; Lin, S. T. The Growth of Structure I Methane Hydrate from Molecular Dynamics Simulations. *J. Phys. Chem. B* **2010**, *114*, 10804–10813.
- (64) Tung, Y. T.; Chen, L. J.; Chen, Y. P.; Lin, S. T. Growth of Structure I Carbon Dioxide Hydrate from Molecular Dynamics Simulations. *J. Phys. Chem. C* **2011**, *115*, 7504–7515.